MAUSAM, **74**, 2 (April, 2023), 287-296

MAUSAM

DOI : https://doi.org/10.54302/mausam.v74i2.5904
Homepage: https://mausamjournal.imd.gov.in/index.php/MAUSAM

UDC No. 551.558.1 : 629.357

Atmospheric convection research using autonomous surface vehicles

KUNIO YONEYAMA, SATORU YOKOI, MIKIKO FUJITA, AYAKO SEIKI,
MASAKI KATSUMATA, BIAO GENG and TATSUYA FUKUDA

Japan Agency for Marine-Earth Science and Technology (JAMSTEC), Yokosuka, Japan

e mail : yoneyamak@jamstec.go.jp

सार – समुद्री महाद्वीप (YMC) के अंतरराष्ट्रीय क्षेत्र कार्यक्रम के तहत, हमने अगस्त-सितंबर 2020 में उष्णकटिबंधीय पश्चिमी प्रशांत महासागर क्षेत्र में 2020 में YMC – बोरियल ग्रीष्मकालीन मॉनसून अध्ययन (YMC-BSM 2020) का एक क्षेत्रीय अभियान चलाया। जबकि इस अभियान का उद्देश्य था एक जहाज और तीन द्वीपों के साथ एक प्रेक्षण सारणी बनाकर बोरियल ग्रीष्मकालीन अन्तरामौसमी दोलन के उत्तर की ओर प्रसार के व्यवहार को प्रेक्षित करना और समझना था, हमने एक महीने के लिए अनुसंधान पोत मिराई के चारों ओर तीन स्वायत्त सतह वाहन (ASVs) और एक सतह उत्प्लव भी तैनात किया। सतह उत्प्लव को न केवल हवा-समुद्र की परस्पर स्थिति का अध्ययन करने के लिए डिज़ाइन किया गया था, बल्कि भविष्य में मेसो-स्केल वायुमंडलीय संवहन अनुसंधान के लिए ASV की क्षमता का विस्तार करने के लिए भी बनाया गया था। इस प्रकार, इस लेख में हम प्रदर्शित करते हैं कि कई ASV में लगे कई उपकरणों की तैनाती संवहन विकास से जुड़ी कुछ बुनियादी वायुमंडलीय विशेषताओं को अन्य मापों द्वारा प्राप्त कई तुलनाओं के साथ प्रेक्षित कर सकती है। 100 किमी के माप के क्रम में कई ASVs को तैनात करना महत्वपूर्ण है, क्योंकि यह सतह के वायुमंडलीय और समुद्री प्राचलों जैसे कि समुद्र की सतह के तापमान की प्रावणता को प्रेक्षित कर सकता है और उनके प्रावणता और वायुमंडलीय संवहन संबंधी विशेषताओं के बीच संबंध प्रदर्शित कर सकता है। चूंकि ASV को छोटे द्वीपों से तैनात किया जा सकता है और किसी भी निर्दिष्ट क्षेत्र पर निगरानी के लिए रिमोट से नियंत्रित किया जा सकता है, यह वायुमंडलीय संवहन का अधिक लचीले ढंग से अध्ययन करने के लिए ASV का भविष्य में उपयोग के लिए शामिल किया जा सकता है।

ABSTRACT. Under the international field program Years of the Maritime Continent (YMC), we conducted a field campaign YMC-Boreal Summer Monsoon study in 2020 (YMC-BSM 2020) in the tropical western Pacific in August-September 2020. While this campaign was aimed to capture and understand the behavior of northward propagating boreal summer intraseasonal oscillation by forming an observation array with a ship and three islands, we also deployed three autonomous surface vehicles (ASVs) and one surface buoy around the research vessel Mirai for one month. The latter was designed not only to study air-sea interaction but also to extend a capability of ASVs for meso-scale atmospheric convection research in future. Thus, in this article we demonstrate that deployment of several instrumented ASVs can capture some basic atmospheric features associated with convection development by showing several comparisons with that obtained by other measurements. Deploying several ASVs in order of 100 km scale is the key, because it can capture gradients of surface atmospheric and oceanic parameters such as sea surface temperatures and can demonstrate a relation between their gradients and atmospheric convection-related features. Since ASVs can be deployed from small islands and controlled remotely to occupy any designated area, this might engage future use of ASVs to study atmospheric convection more flexibly.

Key words – Years of the Maritime Continent - Boreal summer monsoon study in 2020 (YMC-BSM 2020), Autonomous surface vehicle, Meso-scale gradient.

1. Introduction

An international field program called the Years of the Maritime Continent (YMC) has been conducted since 2017 (Yoneyama and Zhang, 2020). YMC is designed to improve our understanding and prediction skill of the weather-climate system over the MC region and its global impact. For this, YMC offers research community coordination opportunities for field campaigns with the MC local agencies and many intensive observations have

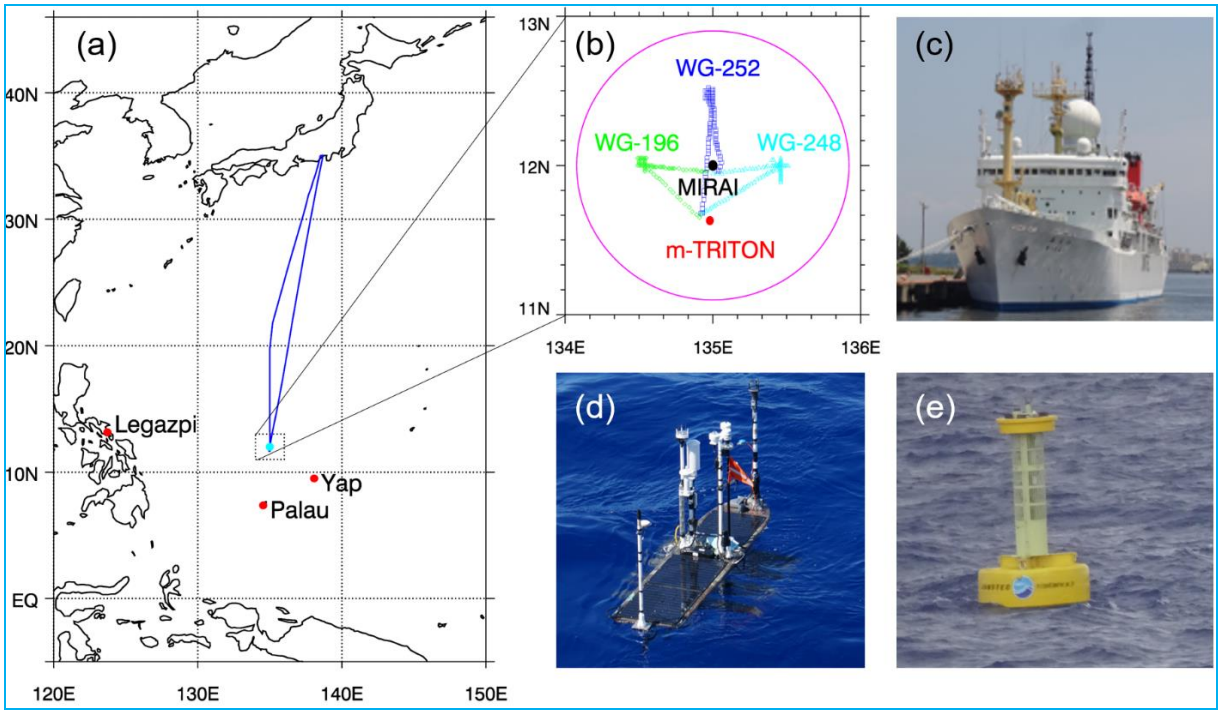

Figs 1(a-e). (a) R/V Mirai cruise track and YMC-BSM 2020 large observation network, (b) configuration of meso-scale observation array, (c) R/V Mirai, (d) wave-glider and (e) m-TRITON buoy. Magenta circle in (b) indicates Doppler radar range (100 km) from the ship. Locations of three ASVs are plotted every hour using different colors/symbols

been carried out focusing on various research topics. They include diurnal cycle of rain, the Madden-Julian Oscillation (MJO), boreal summer intraseasonal oscillation (BSISO), monsoons, interaction among these phenomena and so on. Since several field campaigns have been postponed due to COVID-19 pandemic, its field campaign phase is expected to continue until early 2023. The Japan Agency for Marine-Earth Science and Technology (JAMSTEC) conducted several field campaigns with many local agencies and universities from Indonesia, Philippines, Palau and the Federated States of Micronesia (FSM). One of them is YMC-Boreal Summer Monsoon study in 2020 (YMC-BSM 2020), which aimed at understanding atmospheric convection associated with the BSISO and we conducted a field campaign using the research vessel (R/V) Mirai in August - September 2020. While a radiosonde sounding array was formed by the R/V Mirai and three islands (Legazpi/Philippines, Palau and Yap/FSM) to monitor large-scale atmospheric features with the help from the Department of Science and Technology-Philippine Atmospheric, Geophysical and Astronomical Services Administration (DOST-PAGASA), Palau Weather Service Office, Yap Weather Service Office and the U.S. National Oceanic and Atmospheric Administration (NOAA), a small array consisted of the R/V Mirai, three autonomous surface vehicles (ASVs) and one moored surface buoy was configured to study a relationship between atmospheric convective activity and sea surface condition from meso-scale viewpoint [Figs. 1(a-e)]. The latter was also anticipated to provide a verification of further capability of ASVs for meso-scale atmospheric convection research. This is because while it is desired to deploy various observational platforms such as ships and moorings to form an array for a necessary period to capture targeted phenomena, it is usually very difficult to do so due to the budget constraint and limited human resources. Besides, while researchers usually make an observational plan and decide the observation area based on the previous studies and/or statistical analyses, it does not guarantee that the observation area and campaign period are adequate to capture the targets. The big advantage of ASVs is their flexibility of deployment (though we must care about the international law to conduct any marine scientific research within the exclusive economic zone of any country), which may overcome some above-mentioned difficulties as will be discussed in this article.

Many previous studies emphasized the importance of multi-scale interaction and meso-scale convective systems occupy a large portion of large-scale disturbances and total rainfall over the tropical western Pacific warm pool

region (Mapes, 1993; Katsumata and Yoneyama, 2004; Li and Carbone, 2012). Using satellite-based data Li and Carbone (2012) demonstrated a tight relationship between convective rainfall onset and meso-scale sea surface temperature (SST) gradient. In addition, some studies suggested that interaction between large-scale monsoon flow and convective systems might be a key for the northward propagation of the BSISO (Jiang *et al*., 2004; Bellon and Sobel, 2008; Kang *et al*., 2010). Thus, even when we study large-scale phenomena such as BSISO, it is meaningful to obtain knowledge about meso-scale features.

While large-scale atmospheric features can be obtained by satellite-based data, *in situ* observations focusing on meso-scale viewpoint is necessary to reveal their relation and ocean surface conditions should also be observed. When we deploy a research vessel, it can measure various atmospheric and oceanic parameters around the ship. However, it is difficult to obtain data about ocean surface conditions beyond a certain range from the ship. Thus, we adopted ASVs to compensate for this deficiency. In particular, by deploying several ASVs at once, we could measure their gradient as will be discussed later. For the YMC-BSM 2020 campaign, we used "wave-glider" as ASV. The wave-glider manufactured by the Liquid Robotics Inc. (USA), which converts ocean wave motion to propulsion power, is designed and developed to enhance air-sea interaction and upper ocean studies (Hine *et al*., 2009) and its capabilities are well tested and documented in Grare *et al*. (2021). Equipped measuring instruments gain electric power from solar panels mounted on the top of the float [Fig. 1(d)]. Although its power storage and production are limited as it depends on weather conditions, it is possible to attach any measuring instruments in addition to their standard surface meteorological and oceanic measurement systems. Thus, to enhance measurement related to atmospheric convection, we mounted a Global Navigation Satellite System (GNSS) receiver to obtain precipitable water vapor (Fujita *et al*., 2020). Although we could get 1.5-month ship-time to conduct a field campaign as YMC-BSM 2020, we recognize we need to conduct observations in future under the various atmospheric and oceanic conditions such as different El Niño-Southern Oscillation phases to better understand the behavior of BSISO and related atmospheric convection. Thus, comparison among various observational tools such as ship, ASVs and satellite-based data will help future studies when we conduct a campaign using ASVs even without a ship. Deployment of several ASVs around the R/V Mirai was our trial to evaluate how those ASVs capture the atmospheric convective activity, so that it may open a possibility to use them for meso-scale atmospheric convection research in future.

Thus, this article introduces our recent attempt using ASVs to study a relationship between ocean surface condition and atmospheric convection by demonstrating its capability based on the comparison of their results with the features obtained by a shipboard radar, radiosonde sounding and satellite-based data.

2. Data

We deployed the R/V Mirai as a main platform of the YMC-BSM 2020 campaign and we deployed one moored surface buoy system (called m-TRITON) on 7 August, 2020 and released three ASVs on 8 August 2020 at around 11.6° N, 135.0° E. Then, the R/V Mirai occupied a stationary observation site at 12.0° N, 135.0° E for one month since 9 August and three ASVs occupied west (12.0° N, 134.5° E), north (12.5° N, 135.0° E) and east (12.0° N, 135.5° E) apexes of the small array [Fig. 1(b)]. While m-TRITON buoy was recovered at the deployed site on 8 September, three ASVs were recovered at 12.0° N, 135.0° E on 4 September. Note that the three ASVs were designed to keep their positions within a 5 km range from each site and the comparison or calculation using data obtained by these three ASVs were made only when they occupied their sites. Also, since their cruising speed was about 1 knot (1.5-2 km/h) at maximum, hourly data is almost equivalent to 2 km mean values in space.

In this study, we used surface meteorological data from all platforms (ship, ASVs and m-TRITON buoy). They include pressure, air/sea temperatures, relative humidity, rain, wind and short/long-wave radiation (Note. No long-wave radiation sensor for m-TRITON). Although sampling intervals are 6-second for the Mirai and 10-minute for ASVs and m-TRITON, we used hourly-mean data after spike noises were removed. Details of each system and sensor information of the R/V Mirai, ASVs and m-TRITON buoy can be found in the R/V Mirai cruise report (JAMSTEC, 2020). It should be noted that since locations of sea surface temperature sensors in each platform were different (0.2 m depth for ASVs, 1 m for m-TRITON and 5 m for Mirai), when we compared them, we converted their data to ocean skin temperature using the COARE algorithm (Fairall *et al*., 1996, 2003).

Here, one remark on the quality control of ASV data is described. In addition to the standard calibration for measurement sensors at the manufactures, technical staff of the R/V Mirai confirmed sensors' performance and found no significant biases and/or drifts between before and after the cruise. In addition, there was no significant bias among them when three ASVs were deployed and recovered at the same location. Indeed, one reason to deploy and recover those ASVs and stay for several hours at the same location was to obtain the data for comparison.

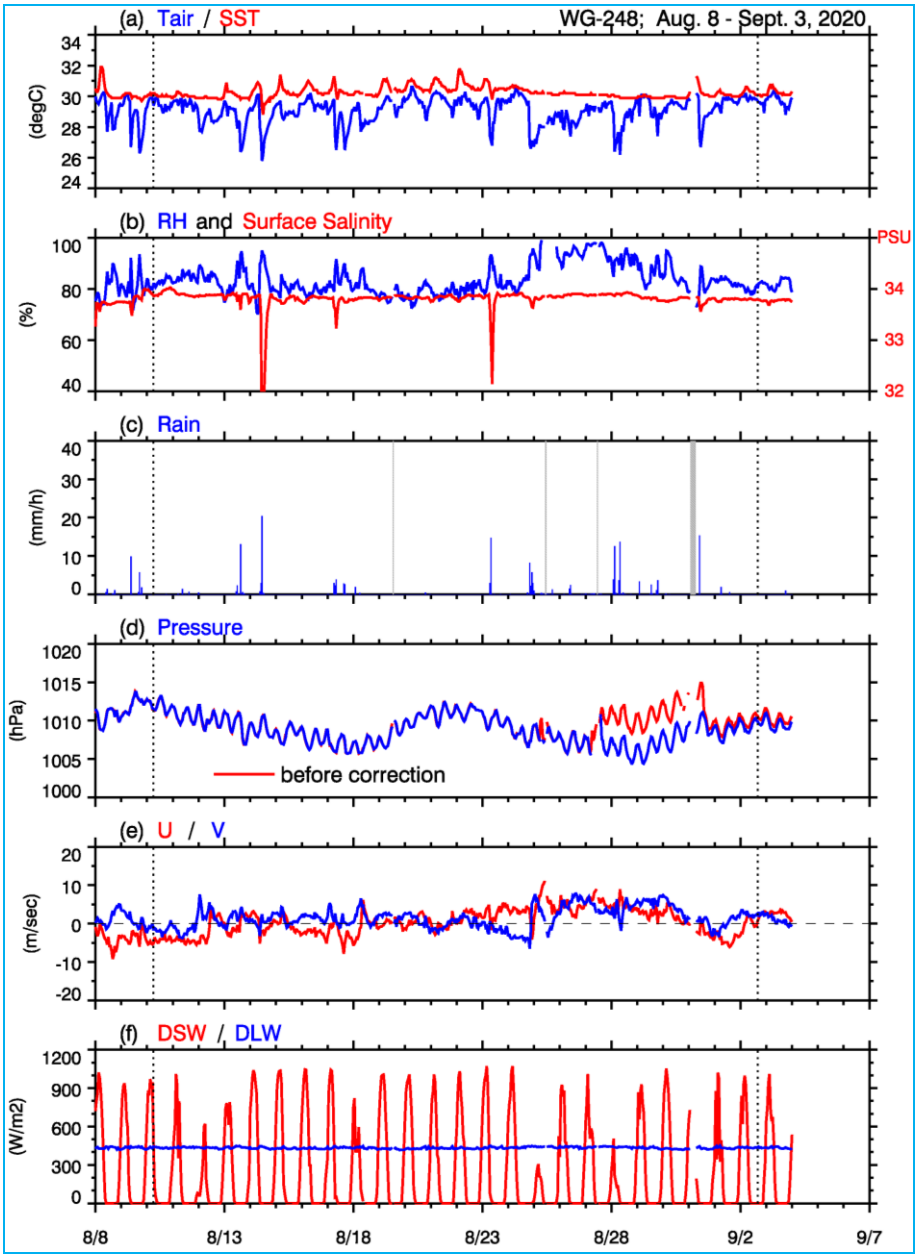

Figs. 2(a-f). Time-series of surface meteorology obtained by one ASV deployed at around 12° N, 135.5° E. (a) air (blue) / sea(red) temperature, (b) relative humidity (blue) and ocean surface salinity (red), (c) rainfall rate, (d) pressure (blue: corrected, red: raw), (e) zonal (red) and meridional (blue) wind components and (f) downward short(red)-/long(blue)-wave radiation. Gray lines in (c) indicate missing data. Vertical dotted lines indicate the start and end of on-station period

Instead, it was found that there was suspicious pressure data obtained by one ASV deployed at the east side of the observation array [WG-248 in Fig. 1(b)] for the period after 27 August. Figs. 2(a-f) show the time series of all surface meteorological data obtained by the ASV WG-248. Abrupt increase and decrease of pressure data can be found in Fig. 2(d) on 27 August and on 31 August, respectively. We speculate such an increase was caused due to water invasion into the barometer system (for example, it might happen due to rough sea conditions). In fact, after the cruise we confirmed that the comparison of three pressure sensors equipped on the ASVs showed the same values within 0.03 hPa accuracy and a shift to high pressure value could be appeared again when a certain

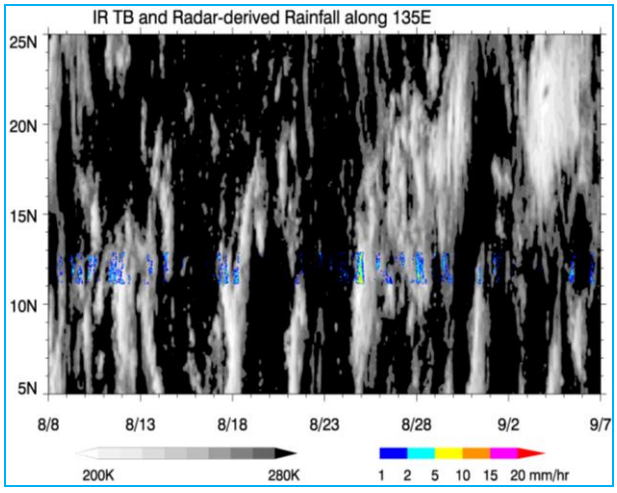

Fig. 3. Time-latitude cross section of IR brightness temperature along 135° E averaged between 134.5° E-135.5° E (monochrome shading) and rain rate estimated from the Mirai radar (color shading)

amount of water was kept in the system until such water was flushed out (we confirmed this manually in the experiment room). To remove this bias, we assumed that synoptic-scale atmospheric condition, which covers the observation area in Fig. 1(b) for several days, might be almost the same. Then, we calculated the mean pressure values during this period for all ASVs and identified 4.0 hPa as a difference with other two ASVs. We also noted that such a difference by 0.7 hPa between 31 August and 3 September. These biases are removed from the original data. Fig. 2(d) demonstrates before and after such bias correction as well as spike noise correction. From this result, we can say that this observation style deploying several ASVs at the same location and then covering O (100 km) area has an advantage for data quality check.

In addition to the standard surface meteorology, to obtain moisture data in the troposphere from all platforms (ship, buoy and three ASVs), we mounted a GNSS receiver, which enables us to calculate precipitable water vapor (PWV). The procedure is the same as that done for another YMC campaign in 2018 (Fujita *et al*., 2020). It is almost impossible to evaluate accuracy of each GNSS-derived PWV, as we do not have independent data to compare at each site. However, as far as we compare their PWV data with that obtained from radiosonde, which ascended within 60 km from all ASV and m-TRITON sites, they show the mean difference better than 2.3 mm (not shown). Thus, at least, they capture moisture variation well like radiosonde data do. Note that although we obtained data with a 10-minute interval, enough sampling for PWV calculation was gained only until 28th August, 2020.

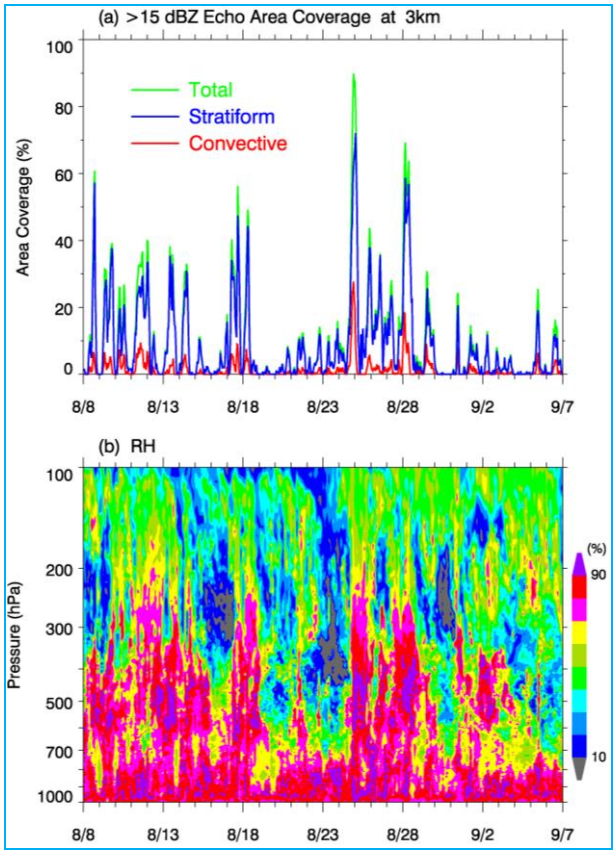

Figs. 4(a&b). (a) Time series of radar echo area coverage whose reflectivity exceeds 15 dBZ for convective (red) and stratiform (blue) types at 3-km height. Green line indicates a sum of convective & stratiform types and (b) Time-height cross section of relative humidity obtained by radiosonde launched from the R/V Mirai every 3 hours

To know atmospheric condition and convective activity during the campaign period, we utilized a vertical profile of relative humidity obtained by 3-hourly radiosonde sounding and C-band polarimetric Doppler radar data taken onboard the R/V Mirai. As for the quality control of radar data, we applied the correction algorithm developed by Geng and Katsumata (2020) to reduce several errors. We utilized radar data sampled hourly (Note. Original data were sampled every 6 minutes) with 1 km/0.5 km resolutions in horizontal/vertical direction within 100 km radius range. When we converted reflectivity data onto rain rate, we adopted a formula provided by Tokay and Short (1996).

We also utilized satellite-based infrared brightness temperature data (NCEP/CPC L3 Half Hourly 4 km Global (60° S-60° N) Merged IR V1) (Janowiak *et al*., 2017) to confirm large-scale cloud activities over our observational area. Data are produced by the U.S. National Oceanic and Atmospheric Administration (NOAA) Climate Prediction

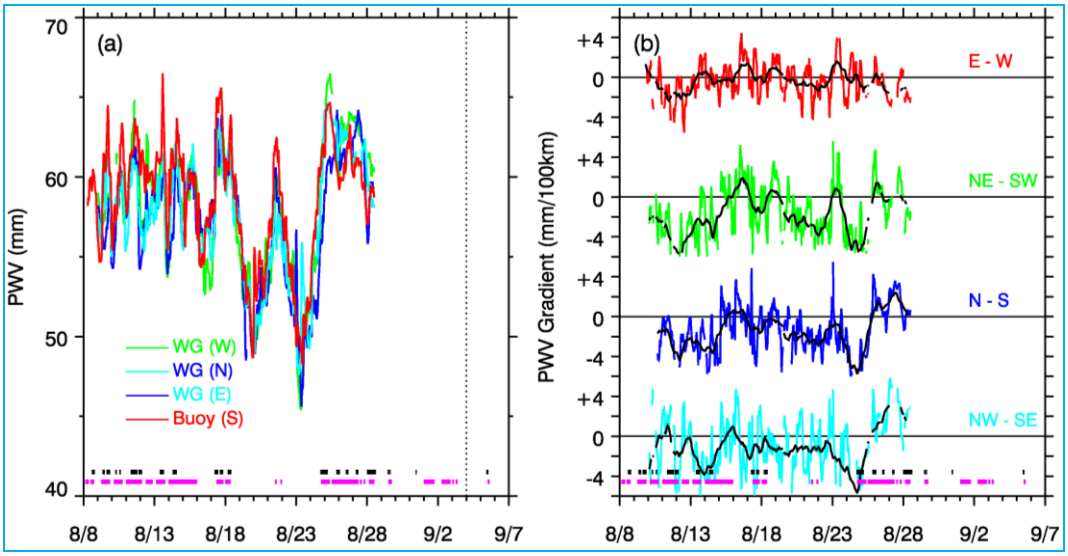

Figs. 5(a&b). (a) Time series of precipitable water vapor obtained at three ASVs and one buoy. (b) Differences of precipitable water vapor in east-west (E-W, red), northeast-southwest (NE-SW, green), north-south (N-S, blue) and northwest-southeast (NW-SE, light blue) directions with respect to 100 km distance. Black line indicates 24-hour moving average. NW, NE, SE and SW components are deduced from the average of two data taken at each ASV deployed at west, north, east and buoy at south (e.g., NW is the average of ASV-north and ASV-west). Horizontal dashed lines near the bottom of both figures indicate the convectively active (black) and moist (magenta) period defined by radar echo area and radiosonde-based PWV

Center and are available from National Aeronautics and Space Administration (NASA) Goddard Earth Sciences Data and Information Services Center.

3. Results and discussion

3.1. *Atmospheric convection features during the campaign period*

Fig. 3 shows the time-latitude cross section of infrared brightness temperature along 135° E. Rainfall rate derived from C-band polarimetric radar is also over plotted. In general, the campaign period was convectively active and large-scale cloud areas appear with a few days interval. Clear northward propagation of such cloud areas can be found twice around 18 August and 24-29 August. Comparison of brightness temperature data with radar-observed rain distribution indicates that convective rain appeared first and then the observation area was covered with stratiform clouds but no significant rain. This situation can be confirmed from a time series of radar echo data with classification into convective and stratiform-types following the technique developed by Steiner *et al*. (1995). Fig. 4(a) shows the time series of echo area coverage and indicates that large portions of stratiform type echo follow the convective ones (*e.g*., August 18, 24, 28 and 29). The time-height cross section of relative humidity obtained by 3-hourly radiosonde from the R/V Mirai shows the corresponding moist condition through the campaign period with some dry intermittent days [Fig. 4(b)].

3.2. *Observations by a small configuration array*

In this sub-section, we demonstrate how and what three ASVs and m-TRITON buoy, which form a meso-scale O (100 km) observation array around the R/V Mirai, capture the atmospheric convective activity, referring the results obtained by a shipboard radar, radiosonde and satellite-based data.

Fig. 5(a) shows the time-series of precipitable water vapor (PWV) derived from GNSS signals. Black and magenta (dashed) lines near the bottom of the figure indicate the periods when the areal coverage of radar echo (> 15 dBZ) exceeds 20% within 100 km radar range (black) and when the PWV derived from radiosonde exceeds 60 mm (magenta). These two lines will be used in the following discussions to refer convectively active and moist periods. GNSS-based PWV captures moist variation well in correspondence with relative humidity data from radiosondes. It can be noted that there is a peak of PWV around 21 August, which is also confirmed in radiosonde data, while radar data do not capture significant rain on that date. From satellite-based cloud distribution (Fig. 3), it is suggested that atmospheric convection exists not over

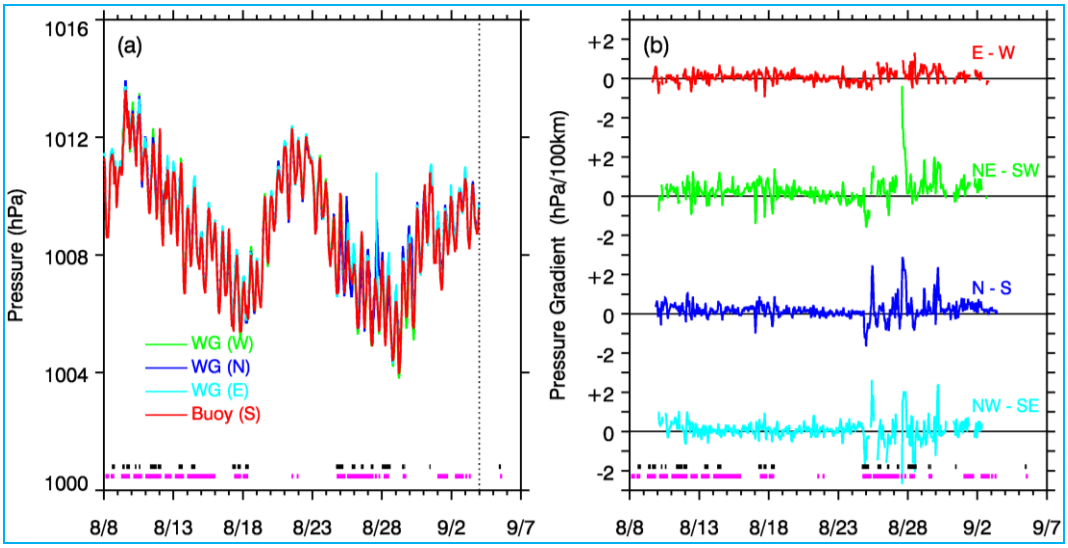

Figs. 6(a&b). Same as Fig. 5, but for surface pressure

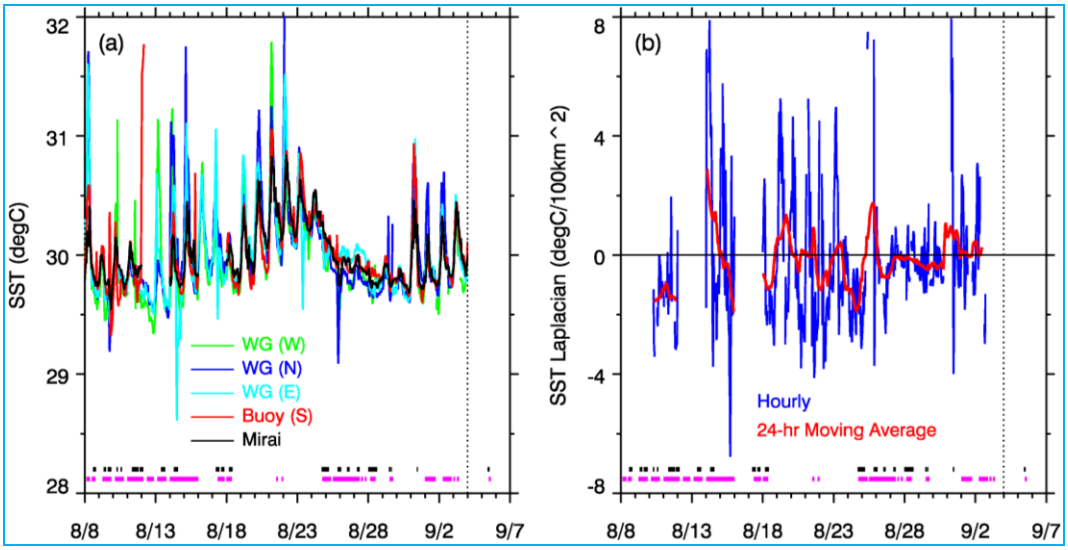

Figs. 7(a&b). (a) Time series of skin SSTs obtained at the R/V Mirai, three ASVs and one buoy. (b) Time series of Laplacian of SST expressed as per 100 km range. Blue and red indicate hourly and 24-hour moving average values, respectively

the radar range but around the site. From the time-longitude cross section of infrared brightness temperature (not shown), cloud area passed over the array from east to west during this period. At least, from the comparison among these figures, we can confirm GNSS-receiver equipped ASV can properly capture lower tropospheric moisture variation. For example, the differences of PWV between four sites [Fig. 5(b)] capture the northward propagation of moist area from 24 August to the following days (only the figures with data taken at the north and south apexes show the variation from negative to positive values) as demonstrated in the satellite-based Fig. 3.

While moisture and radar-derived rain fields indicate frequent (short interval appearance of) moist and convectively active conditions within one month campaign period, pressure field show a different feature. Fig. 6(a) shows the time-series of pressure at four sites and they all show quasi-biweekly oscillation with two low-pressure peaks around 17-18 August and 28-29 August suggesting the passage of synoptic or large-scale disturbances. In particular, pressure gradients among four sites [Fig. 6(b)] demonstrate clear differences especially in the meridional direction. (It should be noted that since data quality discussed at Section 2 is about the ASV

deployed at the eastern apex, their correction scheme and its reliability do not affect this discussion.) These features are consistent with cloud activity derived from satellite-based data as noted in the previous sub-section (Fig. 3), where northward cloud area propagation is observed in these two time slots. We can also confirm that diurnal variation of sea surface temperature (SST) is relatively small during these low-pressure peak periods [Fig. 7(a)]. We can say that deploying several platforms with pressure sensors as well as moisture sensors apart from each other on the order of 100 km is useful to detect different time-scale disturbances.

One of the major reasons why we deployed several platforms around the R/V Mirai was to get information about a relationship between atmospheric convective activity and sea surface condition in the meso-scale viewpoint. In particular, SST is the heart of our interest. Previous studies indicated a relationship between convective rainfall onset and meso-scale SST distribution using satellite-based datasets. Li and Carbone (2012) pointed out that rainfall onset is not proportional to SST variation linearly. Instead, rainfall events prefer to occur around 29.5 °C and occur at locations with enhanced horizontal convergence, which is inferred by the Laplacian of SST and where SST Laplacian is negative on the previous day of the event. Negative Laplacian means there is an SST peak within a calculated area. Thus, to study their relation in terms of meso-scale viewpoint, we need to deploy each platform apart from each other at least 100 km or so. Since we have five data sources from three ASVs and one buoy in addition to the ship, we can calculate SST Laplacian. The results are shown in Fig. 7(b). Although it is almost impossible to deduce a statistical relationship due to limited sampling numbers, several points can be confirmed. During 19-23 August, when the pressure gradient among four sites does not change much [Fig. 6(b)] and the amplitude of the diurnal cycle of SST is large [Fig. 7(a)], SST Laplacian also shows a clear diurnal cycle with positive (around local noon) and negative (around local evening) peaks [Fig. 7(b)]. Except this period, when relatively larger variations are found in the pressure gradient in Fig. 6(b) (August 17-18 and 25-28), SST Laplacian show negative values in general. Thus, both might show similar behavior in terms of synoptic (or several days)-scale disturbances, but a clear relation for shorter scale is unclear. Before the appearance of strong convection on 24 August, SST Laplacian showed clear negative values suggesting favorable conditions for development of atmospheric convection. From moisture distribution derived from PWV at four sites [Fig. 5(b)], moist air mass seemed to be located over the southern portion. Then, a large positive value appeared on the following day. This behavior is consistent with the case Li and Carbone (2012) showed. In

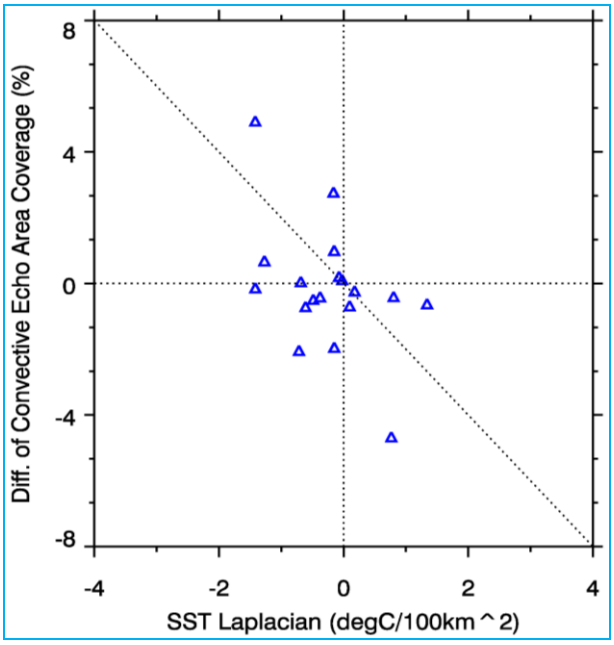

Fig. 8. Scatter diagram of 24-hour mean SST Laplacian and change (difference from previous 24-hour mean value) of 24-hour mean convective echo area coverage. The average period of 24-hour for echo area is behind 12hours for the SST Laplacian

general, 24-hour moving average values show negative in the following several days, when the radar echo and satellite-derived convection indices indicate it was convectively active period. To demonstrate their relation quantitatively, a scatter plot was made. Fig. 8 indicates a relationship between the 24-hour mean SST Laplacian and convective echo area variation. We calculated the change of 24-hour mean convective echo area coverage from previous day as an index of convection onset. In addition, since we confirmed SST Laplacian proceeds echo area variation about half day based on their lag-correlation (not shown here, weak but statistically significant), we calculated 24-hour mean value for radar echo data by 12-hour behind that for SST Laplacian. We have 18-day samples. Although a linear relation between SST Laplacian and convection onset is not necessary as convections are caused by various factors, Fig. 8 shows a correlation (-0.49), which is statistically significant. At least, it is worth noting that positive increments of convective echo area appear only SST Laplacian half day before is negative. Next, to see a relation of SST Laplacian-derived divergence field with actual wind-derived one, we calculated mass divergence and vorticity at the ocean surface horizontal plane using surface wind data [Fig. 9(a)]. It should be noted that since we have only data at the ocean surface, the results may still contain possible observational errors as we cannot eliminate them. However, at least qualitatively Fig. 9(b) supports several

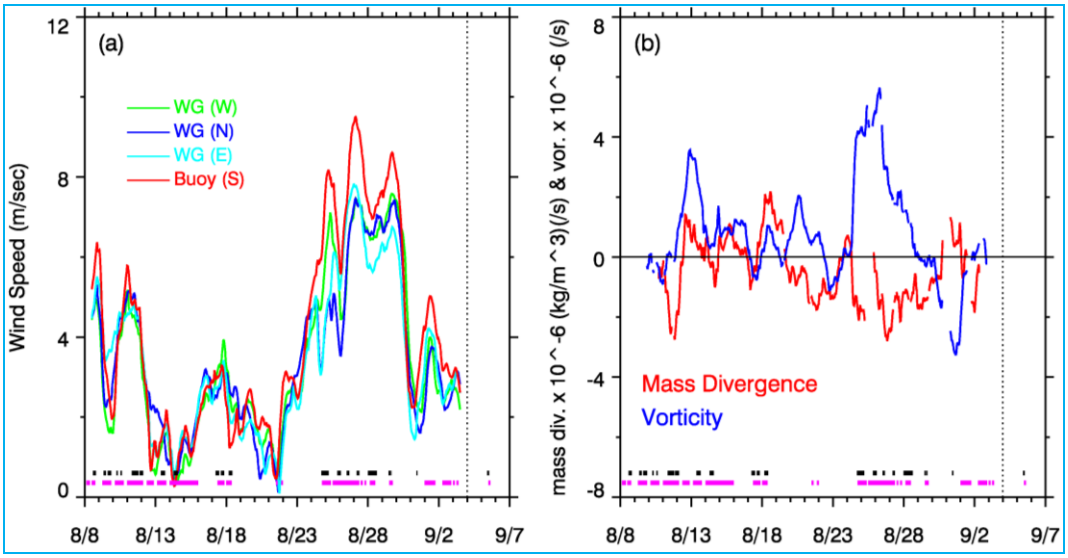

Figs. 9(a&b). (a) Same as Fig. 5(a), but for 24-hour moving average wind speed and (b) Time series of mass divergence and vorticity calculated at the surface

features obtained by other parameters. A time-series of mass divergence indicates favorable condition for convection development during 19-29 August (except from late 23 to early 24 August) and positive (cyclonic) vorticity can be found when large cloud system appeared over the region during 24-28 August. A negative peak of SST Laplacian [found in Fig. 7(b)] appeared half a day or so earlier than the convectively favorable wind-derived pattern (low level convergence and cyclonic flow). SST Laplacian-derived divergence should have a tight [and linear under certain conditions such as that the mesoscale temperature/pressure gradients are small above the top of the mixed layer as noted by Li and Carbone (2012)] relationship with actual divergence field. Comparing SST Laplacian [Fig. 7(b)] with divergence field [Fig. 9(b)], although a significant correlation is not found, we can confirm an agreement of the sign of divergence over 64% during the campaign period. Their detailed relationship remains as a future study to identify the role of meso-scale SST gradient.

4. Conclusions

During the field campaign YMC-BSM 2020, three ASVs and one surface buoy were deployed roughly 50 km away from the R/V Mirai at 12° N, 135° E and they occupied each position about one month to study air-sea interaction as a part of the boreal summer intraseasonal oscillation research. This configuration was also meant to evaluate and expand a capability of instrumented ASVs for future studies on atmospheric convection from the meso-scale viewpoint. This article introduced the latter.

A small configuration array with those ASVs successfully captured several specific features associated with atmospheric convection. First, GNSS-derived PWV demonstrated moisture variation well in accordance with humidity variation observed by radiosonde sounding. At this moment, information about integrated values is obtained and they basically represent a moisture condition in the lower troposphere. However, since cumulus-type clouds develop first over the tropical Oceans and then most stratiform clouds follow to develop (e.g., Houze, 2004), PWV and its variation provide key information for atmospheric convection development. Second, the pressure field can be a good indicator of synoptic-scale and/or large-scale variation and help distinguish from small disturbances. Third, by deploying ASVs apart from each other on the order of 100 km, it might be possible to deduce a relationship between SST gradient and atmospheric convective activity. Since the current study captured only a few examples, long-time observations are required under the various weather/sea conditions to deduce their actual relation. But, at least, we confirmed that negative SST Laplacian corresponded with convection development for the certain period as found in the past studies (Li and Carbone, 2012). Finally, divergence and vorticity fields are in general consistent with convective activity deduced from satellite-based cloud activity. Further detailed comparison of divergence fields derived from SST Laplacian and from wind data is required to deduce the role of SST distribution onto the convective development. Since the current research is our first step to verify the usefulness of deploying several ASVs over the Ocean from the meso-scale viewpoint, we

only showed general features and compared with data obtained by instruments equipped onboard the ship as well as satellite-based data. Since we obtained plenty of observations including C-band polarimetric Doppler radar and 3-hourly radiosonde soundings, thermodynamic and dynamic fields [Figs. 7(a&b) and 9(a&b)] will be intensively studied using those data as a next step. This may support and provide further evidence of usefulness of autonomous vehicle as a platform for observations and also indicate the points needed to be improved. In addition, although we introduced a case obtained over the open ocean, such deployments near the coast must be useful to study air-sea-land interactions by combining land-based observations. Thus, through the knowledge obtained by the YMC program, which focus on the weather-climate system over the Maritime Continent, we anticipate that unique usage of ASVs would be proposed in future.

Finally, it should be noted that *in situ* data obtained during the YMC-BSM 2020 campaign including ASV data used in this study are available from the YMC data site at https://www.jamstec.go.jp/ymc/ymc_data.html.

Acknowledgements

The authors would like to express their sincere thanks to all ship crew of the R/V Mirai and technical staff from Nippon Marine Enterprise Ltd. and Marine Works Japan Ltd. (MWJ) for conducting all observations successfully including data quality control procedures before/after the cruise. In addition, ground supporting staff from MWJ provided skillful maneuvers of wave-glider operation during the entire one month. Comments from the reviewer were also very helpful to improve the manuscript. IR brightness temperature data produced at the NOAA Climate Prediction Center were obtained from the NASA Earthdata site (https://disc.gsfc.nasa.gov/datasets/GPM_MERGIR_1/summary).

Disclaimer : The contents and views expressed in this study are the views of the authors and do not necessarily reflect the views of the organizations they belong to.

References

Bellon, G. and Sobel, A. H., 2008, "Instability of the axisymmetric monsoon flow and intraseasonal oscillation", *J. Geophys. Res.*, **113**(D7), D07108.

Fairall, C. W., Bradley, E. F. , Godfrey, J. S., Wick, G. A., Edson, J. B. and Young, G. S., 1996, "Cool-skin and warm-layer effects on sea surface temperature", *J. Geophys. Res.*, **101**(C1), 1295-1308.

Fairall, C. W., Bradley, E. F., Hare, J. E., Grachev, A. A. and Edson, J. B., 2003, "Bulk parameterization of air-sea fluxes: Updates and verification for the COARE algorithm", *J. Climate*, **16**, 4, 571-591.

Fujita, M., Fukuda, T., Ueki, I., Moteki, Q., Ushiyama, T. and Yoneyama, K., 2020, "Experimental observations of precipitable water vapor over the open ocean collected by autonomous surface vehicles for real-time monitoring applications", *SOLA*, **16A**, 19-24.

Geng, B. and Katsumata, M., 2020, "An algorithm for detecting and removing the spurious differential phase observed by C-band polarimetric radar in the rain", *J. Meteor. Soc. Japan*, **98**, 3, 585-613.

Grare, L., Statom, N. M., Pizzo, N. and Lenain, N., 2021, "Instrumented wave gliders for air-sea interaction and upper ocean research", *Front. Mar. Sci.*, **8**. doi : 10.3389/fmars.2021.664728.

Hine, R., Willcox, S., Hine, G. and Richardson, T., 2009, "The wave glider: a wave-powered autonomous marine vehicle", OCEANS 2009, Biloxi, MS, 1-6. doi : 10.23919/OCEANS. 2009.5422129.

Houze, R. A., Jr., 2004, "Mesoscale convective systems", *Rev. Geophys*., **42**, 4, RG4003.

JAMSTEC, 2020, "R/V Mirai cruise report MR20-E01", 197 pp. available at https://www.jamstec.go.jp/dcop/e/publications/pdf/CruiseReport_MR20-E01_all.pdf (accessed: 30 April, 2022).

Janowiak, J., Joyce, B. and Xie, P., 2017, "NCEP/CPC L3 Half Hourly 4km Global (60S - 60N) Merged IR V1", A. Savtchenko, Ed., Greenbelt, MD, Goddard Earth Sciences Data and Information Services Center (GES-DISC). doi : 10.5067/P4HZB9N27EKU, (Accessed: February 2022).

Jiang, X. N., Li, T. and Wang, B., 2004, "Structures and mechanisms of the northward propagating boreal summer intraseasonal oscillation", *J. Climate*, **17**, 5, 1022-1039.

Kang, I. S., Kim, D. and Kug, J. S., 2010, "Mechanism for northward propagation of boreal summer intraseasonal oscillation: Convective momentum transport", *Geophys. Res. Lett.*, **37**, 24, L24804.

Katsumata, M. and Yoneyama, K., 2004, "Internal structure of ITCZ mesoscale convective systems and related environmental factors in the western Pacific : An observational case study", *J. Meteor. Soc. Japan*, **82**, 4, 1035-1056.

Li, Y. and Carbone, R. E., 2012, "Excitation of rainfall over the tropical western Pacific", *J. Atmos. Sci.*, **69**, 10, 2983-2994.

Mapes, B. E., 1993, "Gregarious tropical convection", *J. Atmos. Sci*., **50**, 13, 2026-2037.

Steiner, M., Houze, R. A., Jr. and Yuter, S. E., 1995, "Climatological characterization of three- dimensional storm structure from operational radar and rain gauge data", *J. Appl. Meteor*., **34**, 9, 1978-2007.

Tokay, A. and Short, D. A., 1996, "Evidence from tropical raindrop spectra of the origin of rain from stratiform versus convective clouds", *J. Appl. Meteor*., **35**, 3, 355-371.

Yoneyama, K. and Zhang, C., 2020, "Years of the Maritime Continent", *Geophys. Res. Lett*., **47**, 12, e2020GL087182.